AJNR

MR and proton spectroscopy of white matter disease induced by high-dose chemotherapy with bone marrow transplant in advanced breast carcinoma.

M S Brown, J H Simon, S M Stemmer, J C Stears, A Scherzinger, P J Cagnoni and R B Jones

AJNR Am J Neuroradiol 1995, 16 (10) 2013-2020
http://www.ajnr.org/content/16/10/2013

MR and Proton Spectroscopy of White Matter Disease Induced by High-Dose Chemotherapy with Bone Marrow Transplant in Advanced Breast Carcinoma

Mark S. Brown, Jack H. Simon, Salomon M. Stemmer, John C. Stears, Ann Scherzinger, Pablo J. Cagnoni, and Roy B. Jones

PURPOSE: To determine whether the MR-detectable white matter changes associated with high-dose chemotherapy and bone marrow transplant in patients with advanced breast carcinoma are accompanied by neurochemical disturbances detectable by proton MR spectroscopy. **METHODS:** MR studies were obtained in 13 patients, and single-voxel proton MR spectra were acquired in vivo in 12 of these 13 for comparison with 13 age- and sex-matched control subjects. **RESULTS:** Considerable white matter change determined with MR was found in 10 of 13 patients with volume white matter change ranging from 1 to 153 cm^3 (mean, 49 cm^3; SD, 50 cm^3). Single-voxel spectra successfully acquired in 12 patients revealed no significant difference in patients compared with control subjects for the spectral ratios *N*-acetyl aspartate to creatine or *N*-acetyl aspartate to choline at either short or long echo times (30 and 136 milliseconds). **CONCLUSION:** Extensive, late-stage white matter change induced by high-dose chemotherapy is not accompanied by measurable disturbances in the putative neuronal marker *N*-acetyl aspartate, suggesting that chemotherapy-induced white matter disease is predominantly a water space and possibly an extraneuronal process rather than a primary neuronal (axonal) disease. The MR spectroscopic examination, accomplished at the time of the MR imaging examination, complements the MR imaging study by increasing the specificity of the MR-based clinical evaluation.

Index terms: Chemotherapy; Magnetic resonance, spectroscopy; White matter, diseases; Bone marrow transplantation; Carcinoma

AJNR Am J Neuroradiol 16:2013–2020, November 1995

Advances in chemotherapy for breast and other cancers have significantly reduced mortality rates but are increasingly associated with iatrogenic toxicities, including pulmonary (1, 2) and neurotoxicity (3–5). After the original descriptions of methotrexate leukoencephalopathy in the 1970s and early 1980s (4–6), the incidence of cancer treatment–related neurotoxicity seemed to decline but did not completely disappear. More recently, chemotherapy-induced neurotoxicity has assumed even greater importance as approaches such as bone marrow rescue (bone marrow transplant) allow treatment using otherwise supralethal doses of chemotherapeutic agents.

The primary cerebral toxicity of high-dose chemotherapy, with or without radiation therapy, is on the white matter. Chemotherapy-induced leukoencephalopathy or white matter changes have been described most frequently for methotrexate (7–9) and carmustine (BCNU) (10–11), and in our experience, not uncommonly in patients with stage II through IV breast cancer treated with high-dose chemotherapy consisting of carmustine and cisplatin, cyclophosphamide, and bone marrow rescue (12). Despite the extensive T2-weighted imaging–detected white matter involvement, the majority of these white matter changes seem to be clini-

Received February 3, 1995; accepted after revision May 31.

Supported in part by a research grant from General Electric Medical Systems.

From the Department of Radiology (M.S.B., J.H.S., J.C.S., A.S.) and the Bone Marrow Transplant Program (S.M.S., P.C., R.B.J.), University of Colorado Health Sciences Center, Denver.

Address reprint requests to Mark S. Brown, PhD, Department of Radiology, University of Colorado Health Sciences Center, 4200 E 9th Ave, Box A034, Denver, CO 80262.

AJNR 16:2013–2020, Nov 1995 0195-6108/95/1610–2013

cally silent to gross-disease neurologic examination (12). This is similar to other white matter diseases such as multiple sclerosis (13). There is, however, reason to believe that more-sensitive neuropsychologic testing may reveal high-dose chemotherapy–induced abnormalities of cognition, memory, and information processing (14), and transient neurologic events including vision disturbances have been observed (12).

The clinical significance of these white matter changes is not known. They may represent effects that could be an indication that limiting neurotoxic doses of chemotherapy have been reached or exceeded. Alternatively, white matter changes may be sensitive but relatively unimportant signs of chemotherapy effects on the brain that are acceptable byproducts of life-saving therapies. Previous proton magnetic resonance (MR) spectroscopy studies of other white matter diseases such as multiple sclerosis (15–18) and adrenoleukodystrophy (19) have demonstrated significant neurochemical changes compared with normal white matter, suggesting neuronal loss or dysfunction. The purpose of this study was to determine whether high-dose chemotherapy–induced white matter changes are accompanied by similar neurochemical changes.

Materials and Methods

MR imaging studies (n = 13) and MR spectroscopic studies (n = 12) were acquired in female patients (mean age, 47.3 years; SD, 8 years) and 13 age- and sex-matched control subjects (mean age, 42 years; SD, 10) after informed consent was obtained. These patients with stage II through IV breast cancer had been treated with high-dose chemotherapy consisting of cyclophosphamide at 1875 mg/m^2 of patient total body area per day for 3 days as a 1-hour intravenous infusion, cisplatin at 55 mg/m^2 per day as a continuous intravenous infusion for 72 hours, and carmustine at 600 mg/m^2 as a 2-hour intravenous infusion on the fourth day, followed by autologous hematopoietic progenitor stem cell transplant. Before high-dose chemotherapy, induction chemotherapy consisted of multiple cycles of doxorubicin hydrochloride, fluorouracil, and methotrexate. Patients were in some cases exposed to additional chemotherapeutic agents before entrance into the bone marrow transplant program, but none of the patients had prior or subsequent cranial X-irradiation.

Patients in the university bone marrow transplant program were recruited into this MR imaging/MR spectroscopic study from 4 to 21 months after bone marrow transplant (mean, 12 months) and were approached based on the criterion of proximity to the university medical center. Five patients were known to have had white matter changes based on prior MR studies; seven had no prior MR studies and no known or suspected neurologic events after high-dose chemotherapy, although one had been noted to be depressed. An additional patient had a prior negative MR study before induction and high-dose chemotherapy. The MR was acquired as a baseline evaluation for a prospective study, which the patient subsequently withdrew from, and there were no known or suspected clinical events at or subsequent to that MR imaging. Clinical characteristics were confirmed through a retrospective chart review (Table 1).

Control subjects were volunteer healthy subjects with no history of neurologic symptoms or known neurologic disease.

All MR imaging and MR spectroscopic studies were acquired on a 1.5-T Signa system (General Electric Medical Systems, Waukesha, Wis), using a standard bird cage head coil. The imaging protocol included a sagittal localizing image and axial T2-weighted spin-echo sequences (2100/30,90/1 [repetition time/echo time/excitations]), matrix size 256 × 192, section thickness 5 mm with 2-mm gaps, and a 22-cm field of view. Total brain volumes of white matter change were calculated in the patients based

TABLE 1: Patient characteristics, MR imaging/MR spectroscopic timing, and volume data

Patient	Classification	Age, y	Time after HDC, mo	Neurologic Toxicity	Volume WMC, cm^3
1	N	32	9	None	98
2	P	57	17	Psychosis (8 mo), TIA (10 mo)	153
3	P	49	14	TIA (2 mo), Vision (3 mo)	12
4	P	37	21	TIA (9 mo)	87
5	N	50	5	None	12
6	N	49	20	None	1
7	P	39	19	TIA (20 mo)	3
8	P	48	15	Vision (3 mo), TIA (9 mo)	44
9	N	60	11	None	109
10*	N	50	6	None	62
11	N	47	4	None	1
12	Ne	48	10	None	5
13	N	52	11	Depression (6 mo)	51

Note.—P indicates prior positive MR imaging before recruitment; N, no prior MR imaging; Ne, had previous negative MR before bone marrow transplant as part of a prospective study; vision, transient decrease in visual acuity; HDC, high-dose chemotherapy; WMC, white matter change; and TIA, transient ischemic attack.

* No MR spectroscopic study, machine failure.

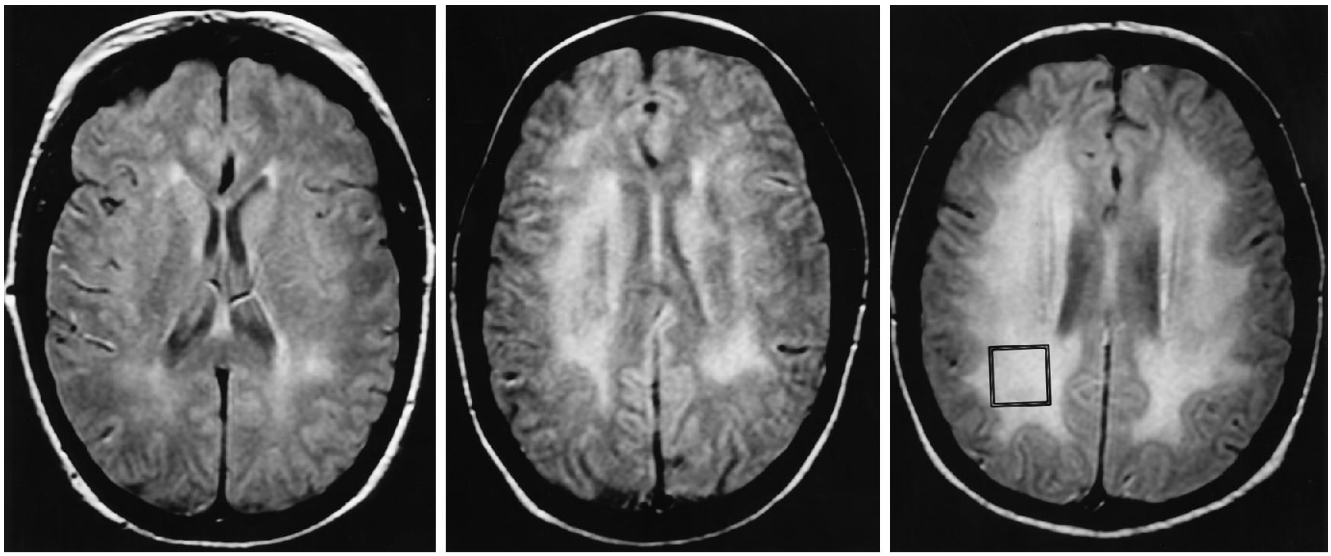

Fig 1. MR imaging results. Representative mild (*A*), moderate (*B*), and severe (*C*) T2 hyperintense white matter change at the level of the lateral ventricle in high-dose chemotherapy–treated patients (patients 5, 10, and 2, Table 1). These corresponded to white matter change volume determinations (white matter change per brain) of 12, 62, and 153 cm^3, respectively. The *box* in *C* indicates the location of the spectroscopy voxel. Spin-echo images with 2100/30.

on a user-interactive semiautomated bifeature space segmentation procedure (20, 21). A neuroradiologist circled the white matter changes on hard-copy film as a guide to the image processing technician. The dual-echo T2-weighted data set was first filtered (21), and then the technician performed the "training function," consisting of ascribing pixels to one of four tissue classes (normal white matter, gray matter, cerebrospinal fluid, and abnormal white matter). Computerized tissue segmentation was based on the Parzen function (22). Finally, the technician used the connectivity function on a section-by-section basis to separate white matter change from cosegmenting normal brain and/or extracranial tissue.

Single-voxel proton spectroscopy was performed on 2 $\times$ 2 $\times$ 2-cm voxels centered in the right (11 studies) or left (1 study) parietal occipital white matter adjacent to the lateral ventricle. This spectroscopy voxel was typically the region of maximal observed white matter T2 hyperintensity. Instrument failure was responsible for the loss of spectra in 1 patient and the loss of the long-echo spectra in 2 patients. Two other patients were unable to tolerate the additional time required for the long-echo acquisition. After shimming to a line width at half height of less than 5 Hz, two spectra of echo times (TEs) of 30 and 136 were acquired using the stimulated-echo acquisition mode pulse sequence (1600/30,136; mixing time, 13.7) with 256 averages preceded by three frequency-selective (chemical shift-selective) water suppression pulses. Data size was 2048 points with a spectral width of 2000 Hz. Processing was performed on a Sun SPARC 2 workstation (Sun Microsystems, Sunnyvale, Calif) using the SA/GE processing software (General Electric Medical Systems) and included zero filling to 4096 points, 0.5-Hz line broadening, Fourier transformation, direct-current offset correction, and manual phasing. The I (real) data channel was extracted, and the residual water peak was fit as a Lorentzian line using the Marquardt fitting routine and subtracted from the spectrum. No additional baseline correction was used. The spectral offset was adjusted so that the large resonance attributed to *N*-acetyl aspartate (NAA) was centered at approximately 2.02 ppm (23). The manual peak-picking routine was used to select resonances at 3.6 ppm attributed to myoinositol (MI), choline-containing compounds at 3.25 ppm (Ch), a creatine/creatine phosphate peak at 3.03 ppm (Cr), and NAA at 2.02 ppm. The resulting peak heights were used to compute ratios between the various metabolites. Ratios were also determined using fitted areas. The spectra were fit with Lorentzian lines using the Marquardt fit algorithm using a total of 17 lines in the TE 30 spectra and 6 lines in the TE 136 spectra, and the resulting fitted areas were used to compute ratios. The protocol for fitting the areas of the peaks was arrived at after extensive investigation involving variation in the number of lines to fit, the line shape, and whether frequency, width, and amplitude were allowed to vary. Lorentzian line shapes were used in the fits, because use of Gaussian line shapes consistently gave larger χ^2 values. Increasing the number of lines in the fits over 17 in TE 30 and 6 in TE 136 spectra gave insignificant reductions in the χ^2 value and often resulted in nonphysical results (eg, negative line widths). The ratios computed from fitted areas nearly always resulted in larger SDs compared with raw peak-picked height ratios, which in our experience show the least operator bias (M. S. Brown et al, unpublished data). Statistical analyses included a two-tailed t test for detection of statistically significant differ-

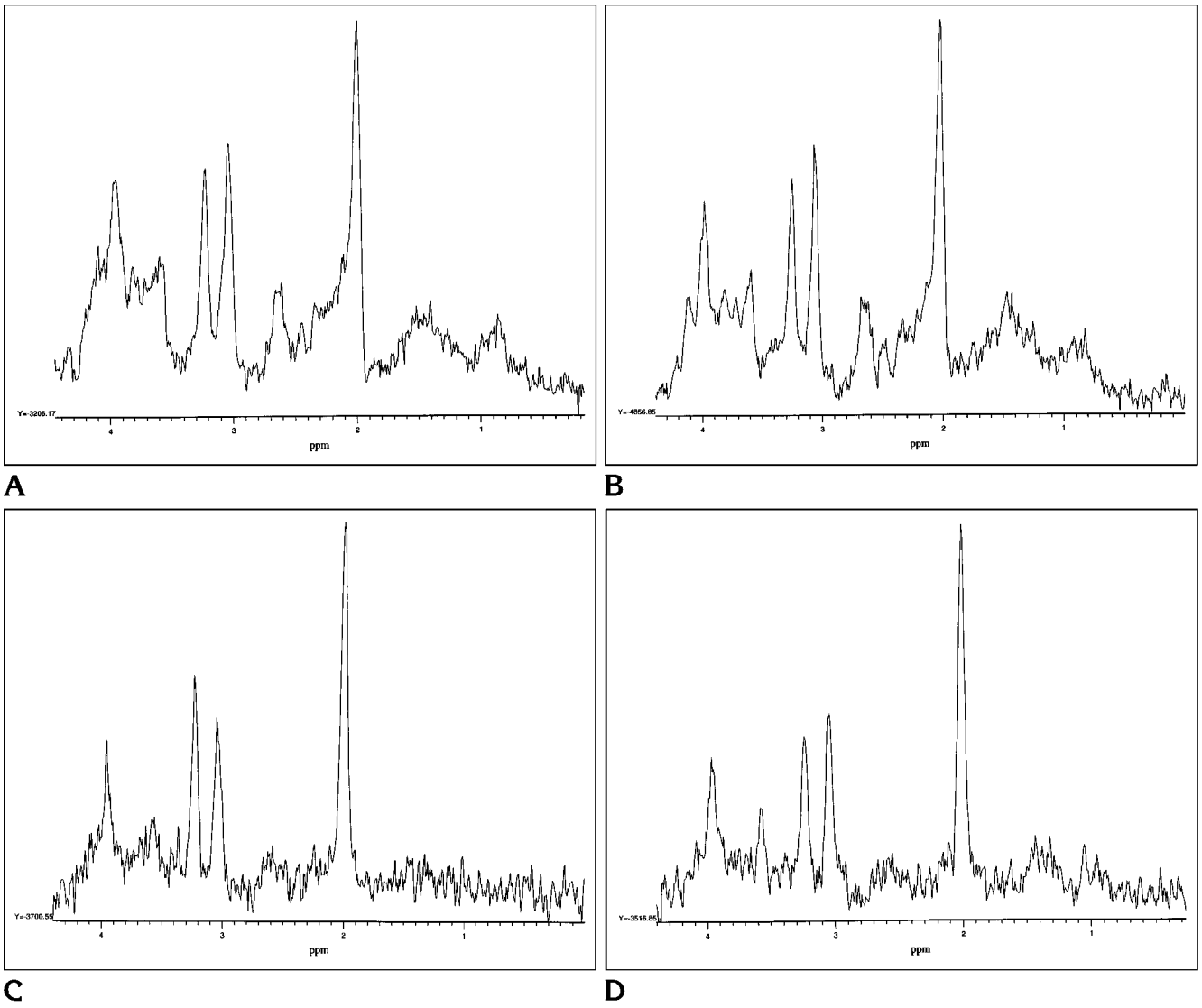

Fig 2. Representative proton MR spectra at TE 30 (*A* and *B*) and 136 (*C* and *D*) in a control subject (*A* and *C*) and the patient with severe white matter changes (patient 2, Table 1) shown in Figure 1C (*B* and *D*). Peak assignments in parts per million (*ppm*) are: NAA, 2.02; Cr, 3.05; Ch, 3.25; and MI, 3.6.

ences between the mean ratios in control subjects and patients and correlation analyses using SPSS (Chicago, Ill) and Excel (Microsoft, Redmond, Wash).

Results

The clinical summary and white matter change volumetric results are presented in Table 1. Transient neurologic events had occurred in all 5 patients with prior clinically indicated MR evaluations, all of whom had white matter changes. The relationship between the neurologic event, principally described as a transient ischemic attack (in four) or psychosis (in one), and the white matter change was not straightforward because of multiple confounding variables (eg, clotting and metabolic status), whereas visual symptoms (in two) were thought to be more directly related to toxic effects on the optic nerve. The subjects without prior post–high-dose chemotherapy MR imaging studies were neurologically normal through the time of the MR imaging/MR spectroscopic evaluation, although one had episodes of depression. White matter T2 hyperintensities ranged from 1 to 153 cm^3 (mean, 49 cm^3; SD, 50 cm^3). There was no apparent correlation between volume of white matter change and neurologic toxicity. In two neurologically negative patients (patients 6 and

11, Table 1), studied at 4 and 20 months after high-dose chemotherapy, small periventricular white matter changes (1 cm^3 in both) were determined by consensus to be more likely related to normal aging than to chemotherapy. Another patient (patient 7, Table 1) with a small volume (3 cm^3) of white matter change thought to be chemotherapy related had a transient ischemic attack–like event at 20 months, as well as major pulmonary complications. The four patients with the most severe white matter changes (>87 cm^3) could be equally divided into symptomatic and asymptomatic groups.

Representative MR imaging results are shown in Figure 1. Typical small-volume white matter changes were scattered predominantly in the posterior periventricular white matter, with progression to confluent white matter change both posterior and anterior, with sparing of the corpus callosum, subcortical *U* fibers, and gray matter, and minimal at the most central or cortical volume loss. Infratentorial findings were confined largely to the peridentate region, as described previously (12).

Except for the two patients judged to have no chemotherapy-induced white matter change (patients 6 and 11, Table 1), the extent of white matter change within the spectroscopy voxel (in the plane-filling factor) ranged from 37.5% to 100% for the patients completing spectroscopy. Representative short- (30-millisecond) and long- (136-millisecond) echo spectra from a control subject and from the patient with severe white matter changes shown in Figure 1C are shown in Figure 2. The spectroscopically determined metabolite ratios NAA/Cr, NAA/Ch, Ch/Cr, and MI/Cr, computed from both peak heights and fitted areas, are summarized in Table 2. Figure 3 shows the distribution of the ratios (using peak heights) between the patients and the control subjects at 30 milliseconds (Fig 3A) and 136 milliseconds (Fig 3B). No statistically significant differences were detected comparing patients and control subjects for mean ratios of the major metabolite markers in either the short- or long-echo spectra. At TE 136 a small increase in MI/Cr was noted to be formally significant ($P = .02$), but because this is one of multiple comparisons, the significance level should probably not be taken literally. Lactate was not detected in patients or control subjects, and only small residual lipid peaks, thought to be normal, were observed in TE 30 spectra in both patients and control subjects. There was no significant correlation between volume of white matter change, age, or time after high-dose chemotherapy and the major spectral ratios.

Discussion

These results indicate that although high-dose chemotherapy is associated with major changes in the white matter, as indicated by MR imaging, by these methods we are unable to detect disturbances in NAA in relatively late stages after high-dose chemotherapy. NAA is generally accepted as a marker of neuronal structure or function (24–28), and therefore the implication of these results is that the observed white matter change is not accompanied by major neuronal and or axonal damage. Using similar spectroscopic methods, significant decreases in NAA have been detected in other white matter diseases, most notably in long-standing multiple sclerosis lesions in the brain (15–18), in which poor voxel-filling factors may in fact underestimate changes, as well as in adrenoleukodystrophy (19). Small decreased levels of NAA have also been reported in both gray

TABLE 2: Proton spectroscopic metabolite ratios in patients and healthy control subjects

Echo Time, ms	Population	n	NAA/Cr Heights	NAA/Cr Areas	NAA/Ch Heights	NAA/Ch Areas	Ch/Cr Heights	Ch/Cr Areas	MI/Cr Heights	MI/Cr Areas
30	Controls	13	1.50 (0.10)	1.21 (0.13)	1.58 (0.20)	1.38 (0.21)	0.96 (0.09)	0.89 (0.13)	0.68 (0.09)	0.54 (0.11)
	Patients	12	1.44 (0.11)	1.30 (0.23)	1.44 (0.17)	1.39 (0.25)	1.01 (0.12)	0.95 (0.18)	0.73 (0.10)	0.61 (0.23)
	Significance		NS	NS	NS	NS	NS	NS	NS	NS
	(*P* value)		.14	.23	.07	.94	.25	.33	.23	.30
136	Controls	13	1.91 (0.18)	1.99 (0.26)	1.80 (0.23)	2.05 (0.41)	1.07 (0.13)	0.99 (0.16)	0.42 (0.09)	0.63 (0.37)
	Patients	8	1.79 (0.17)	1.84 (0.22)	1.72 (0.29)	1.86 (0.29)	1.06 (0.10)	1.02 (0.26)	0.50 (0.05)	0.59 (0.16)
	Significance		NS	NS	NS	NS	NS	NS	S	NS
	(*P* value)		.15	.18	.51	.23	.76	.76	.02	.72

Note.—Values are means with SDs in parenthesis. *P* values determined using two-tailed *t* test with unequal variances. S indicates significant ($P < .05$); NS, not significant.

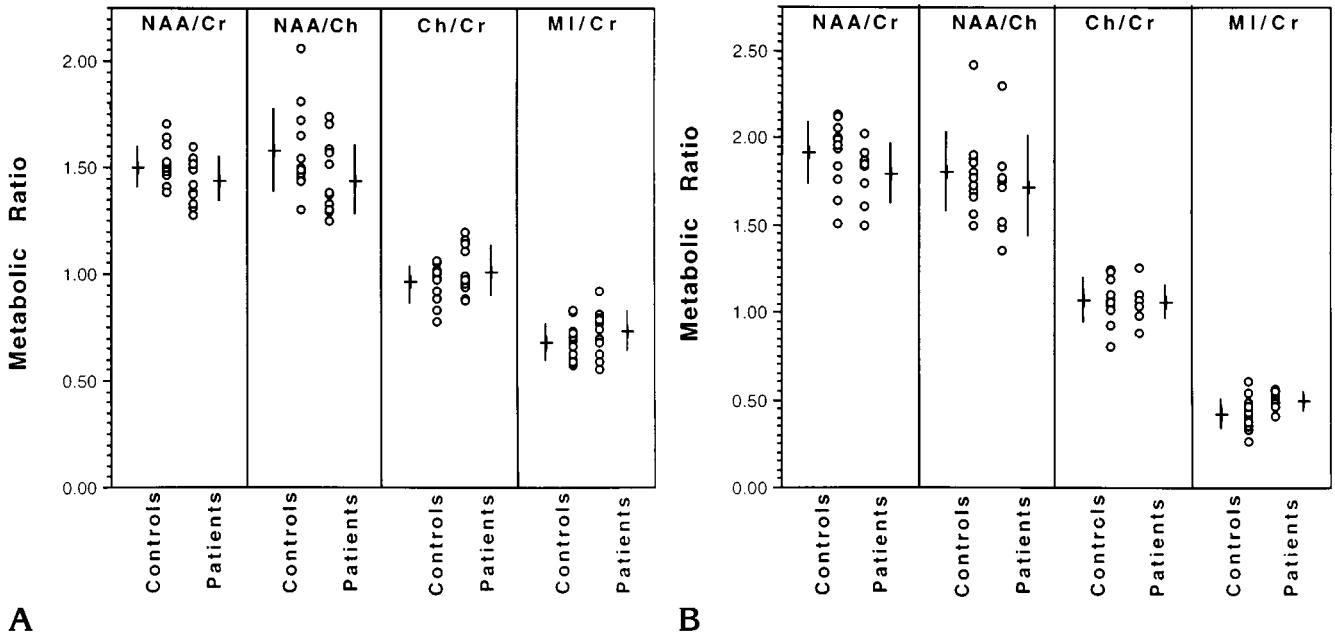

Fig 3. Comparison of proton metabolite ratios from peak heights at *A,* TE 30 and *B,* TE 136. The means (*horizontal line*) and SDs (*vertical line*) are shown, along with measurements for the individual control subjects and patients.

and white matter regions in Alzheimer disease (25, 28), and in cognitively impaired human immunodeficiency virus–seropositive individuals (27). Although this study design may have been insensitive to small decreases in NAA/Cr, the sample size was such that a decrease on the order of 20% could have been detected with a power greater than 99% ($\alpha = 0.05$).

The significance of the small observed changes in the MI/Cr ratio in the long-echo spectra is not known, particularly because of the conflicting results based on interpretation of short-echo and long-echo area-based analyses. The MI peak occurs in a crowded spectral region with many poorly resolved resonances and possible baseline contributions from unsuppressed water. The MI peak is thought to consist principally of MI, with small contributions from inositol 1 phosphate and glycine (28). The role of the MR-detected MI in the brain is not known, although there has been speculation that inositol-containing compounds may function as idiogenic osmolytes in the brain (29) and/or are related to inositol polyphosphate second-messenger metabolism, among other possibilities (28, 30). Elevated levels of MI have been detected by in vivo proton MR spectroscopy in Alzheimer disease (28) and in adrenoleukodystrophy (19).

These combined MR imaging/MR spectroscopic results suggest that high-dose chemotherapy–induced white matter change may not be related to neuronal dysfunction or abnormality but rather reflects changes in the free and bound water fraction as a result of the chemotherapy. The abnormalities detected by intermediate- (long repetition time, short TE) and more T2-weighted spin-echo imaging presumably reflect an elevated T2 relaxation time in a free-water fraction of white matter. Localization of that change to the interstitial spaces and interlamellar spaces (within a disrupted or dispersed myelin membrane), within the glial compartment, or possibly in the intraneuronal space is not currently known. Correlation with histopathologic analysis is available in only one autopsied case, in which the white matter change 24 months after high-dose chemotherapy was associated with patchy, ill-demarcated but diffuse myelin pallor, without the necrosis, vasculopathy, or severe astrocytosis that has been reported in other chemotherapy treatment case studies (11).

The relatively minor changes in the neuronal biochemical milieu detected through MR spectroscopy is consistent with the relatively good level of clinical function and relatively minor or transient neurologic disturbances in these patients (12). Interpretation of the MR imaging findings alone would not have led to a similar conclusion. However, it is important to acknowledge that the retrospective clinical evalu-

ation in this study design will likely lead to an underestimation of significant neurologic impairment. We know, for example, that some patients undergoing high-dose chemotherapy may, in fact, show declining function, in measures of short-term memory, attention, concentration, and information processing speed (A. Futterman et al, unpublished data). Second, these MR spectroscopic results are not relevant to potential changes occurring during the early stages (0 to 3 months) after treatment with high-dose chemotherapy, when white matter change are more likely to be evolving.

The true incidence of high-dose chemotherapy–induced white matter change and the time course for development of these white matter changes is not currently known. Our estimates from this study and our prior retrospective experience suggest that the incidence of white matter change likely exceeds 50%, and that these changes will occur as early as 1 to 3 months after high-dose chemotherapy. At our university medical center alone, more than 100 patients with breast cancer are treated by this approach per year. This and similar aggressive approaches to treatment of advanced breast carcinoma has resulted in decreased mortality rates (2) and is expected to remain the method of choice for treatment of advanced breast carcinoma in many centers supporting a bone marrow transplant program. It is expected that as new high-dose chemotherapeutic regimens are implemented, they may produce different neurotoxicities and MR imaging/MR spectroscopic patterns of brain abnormalities.

Several important questions remain unanswered, which can only be addressed by a prospective longitudinal evaluation of MR imaging/MR spectroscopy and neuropsychologic changes accompanying chemotherapy-induced white matter change. This study suggests that both a morphologic and water-based assay (MR imaging) and a biochemical evaluation by MR spectroscopy may contribute to our understanding these white matter changes, the significance of these white matter changes to the patient, and the impact of these white matter changes on the design of future chemotherapy approaches to treating cancer.

Acknowledgment

We thank Philip Archer, ScD, professor of biometrics, for reviewing the manuscript.

References

1. Jones RB, Matthes S, Shpall EJ, et al. Acute lung injury following treatment with high dose cyclophosphamide, cisplatin, and carmustine: pharmacodynamic evaluation of carmustine. *J Natl Cancer Inst* 1993;85:640–647
2. Peters WP, Ross M, Vredenburgh JJ, et al. High dose chemotherapy and autologous bone marrow support as consolidation after standard dose adjuvant therapy for high risk primary breast cancer. *J Clin Oncol* 1993;11:1132–1143
3. Allen JC, Rosen G, Mehta BM, Horten B. Leukoencephalopathy following high dose IV methotrexate chemotherapy with leucovorin rescue. *Cancer Treat Rep* 1980;64:1261–1273
4. DeAngelis LM, Shapiro WR. Drug/radiation interactions and central nervous system injury. In: Gutin PH, Leibel SA, Sheline GE, eds. *Radiation Injury to the Nervous System*. New York: Raven Press, 1991:361–382
5. Kaplan RS, Wiernik PH. Neurotoxicity of antineoplastic drugs. *Semin Oncol* 1982;9:103–130
6. Peylan Ramu N, Poplack DG, Pizzo PA, Adornato BT, DiChiro G. Abnormal CT scans of the brain in asymptomatic children with acute lymphocytic leukemia after prophylactic treatment of the central nervous system with radiation and intrathecal chemotherapy. *N Engl J Med* 1978;298:815–818
7. Ebner F, Ranner G, Slavc I, et al. MR findings in methotrexate-induced CNS abnormalities. *AJNR Am J Neuroradiol* 1989;10:959–964
8. Lien HH, Blomlie V, Saeter G, Solheim O, Fossa SD. Osteogenic sarcoma: MR signal abnormalities of the brain in asymptomatic patients treated with high dose methotrexate. *Radiology* 1991;179:547–550
9. Abelson HT. Methotrexate and central nervous system toxicity (commentary). *Cancer Treat Rep* 1978;62:1999–2001
10. Burger PC, Kamenar E, Schold SC, Fay JW, Phillips GL, Herzig GP. Encephalomyelopathy following high dose BCNU therapy. *Cancer* 1981;48:1318–1327
11. Kleinschmidt DeMasters BK, Geier JM. Pathology of high dose intraarterial BCNU. *Surg Neurol* 1989;31:435–443
12. Stemmer SM, Stears JS, Burton BS, Jones RB, Simon JH. White matter changes in patients with breast cancer treated with high dose chemotherapy and autologous bone marrow support. *AJNR Am J Neuroradiol* 1994;15:1267–1273
13. Simon JS. Neuroimaging of multiple sclerosis. *Neuroimaging Clin North Am* 1993;3:229–246
14. Andrykowski MA, Altmaier EM, Barnett RL, Burish TG, Gingrich R, Henslee-Downey PJ. Cognitive dysfunction in adult survivors of allogeneic marrow transplantation: relationship to dose of total body irradiation. *Bone Marrow Transplant* 1990;6:269–276
15. Grossman RI, Lenkinski RE, Ramer KN, Gonzalez Scarano F, Cohen JA. MR proton spectroscopy in multiple sclerosis. *AJNR Am J Neuroradiol* 11992;13:1535–1543
16. Larsson HBW, Christiansen P, Jensen M, et al. Localized in vivo proton spectroscopy in the brain of patients with multiple sclerosis. *Magn Reson Med* 1991;22:23–31
17. Matthews PM, Francis G, Antel J, Arnold DL. Proton magnetic resonance spectroscopy for metabolic characterization of plaques in multiple sclerosis. *Neurology* 1991;41:1251–1256
18. Van Hecke P, Marchal G, Johannik K, et al. Human brain proton localized NMR spectroscopy in multiple sclerosis. *Magn Reson Med* 1991;18:199–206
19. Tzika AA, Ball WS, Vigneron DB, Dunn RS, Nelson SJ, Kirks DR. Childhood adrenoleukodystrophy: assessment with proton MR spectroscopy. *Radiology* 1993;189:467–480

20. Cline HE, Lorensen WE, Kikinis R, Jolesz F. Three dimensional segmentation of MR images of the head using probability and connectivity. *J Comput Assist Tomogr* 1990;14:1037–1045
21. Kikinis R, Shenton ME, Gerig G, et al. Routine quantitative analysis of brain and cerebrospinal fluid spaces with MR Imaging. *J Magn Reson Imaging* 1992;2:619–629
22. Duda RO, Hart PE. *Pattern Classification and Scene Analysis*. New York: John Wiley and Sons, 1973:85–129
23. Kreis R, Ross BD. Cerebral metabolite disturbances in patients with subacute and chronic diabetes mellitus: detection with proton MR spectroscopy. *Radiology* 1992;184:123–130
24. Birken DL, Oldendorf WH. *N*-acetyl-L-aspartic acid: a literature review of a compound prominent in ^{1}H NMR spectroscopic studies of brain. *Neurosci Biobehav Rev* 1989;13:23–31
25. Klunk WE, Panchalingam K, Moossy J, McClure RJ, Pettegrew JW. *N*-acetyl-L-aspartate and other amino acid metabolites in Alzheimer's disease brain: a preliminary proton nuclear magnetic resonance study. *Neurology* 1992;42:1578–1585
26. Miller BL. A review of chemical issues in ^{1}H NMR spectroscopy: *N*-acetyl-L-aspartate, creatine and choline. *NMR Biomed* 1991;4: 47–52
27. Meyerhoff DJ, MacKay S, Bachman L, et al. Reduced brain *N*-acetylaspartate suggests neuronal loss in cognitively impaired human immunodeficiency virus seropositive individuals: in vivo ^{1}H magnetic resonance spectroscopic imaging. *Neurology* 1993; 43:509–515
28. Miller BL, Moats RA, Shonk T, Ernst T, Woolley S, Ross BD. Alzheimer disease: depiction of increased cerebral Myo inositol with proton MR spectroscopy. *Radiology* 1993;187:433–437
29. Lien YHH, Shapiro JI, Chan L. Effects of hypernatremia on organic brain osmoles. *J Clin Invest* 1990;85:1427–1435
30. Berridge M. Inositol triphosphate and diacylglycerol as second messengers. *Biochem J* 1984;220:345–360